Cume 386 is based in part on the paper "Excitation Temperature of the Warm Neutral Medium as a New Probe of the Lyman alpha Radiation Field", by Murray et al., 2014, ApJ 781, L41.

<u>Note</u>: you do not need to read the entire paper for this cume. The most relevant parts are the Abstract, Introduction, and Section 2.1. The exact nature of the stacking and fitting of the spectra in Section 2.2 and Section 3 is not relevant for answering the questions. Section 4 may be useful to better understand the main message of the paper.

The total number of points is 85. The passing grade is expected to be 70%. Many of the questions are general questions regarding radiative transfer and the atomic hydrogen in the ISM.

Question 1: 5 short questions 25 pts

Question 2: Discussion of Lyman  $\alpha$  emission, 15 pts Question 3: HI emission and absorption spectra, 45 pts

1. First some short questions.

1a. (5 pts) Calculate the frequency of the HI 21-cm line. Calculate the beam size of the 1000-ft Arecibo dish at this wavelength.

- 1b. (5 pts) What quantity is the "Jansky" a unit of? Write out what a Jansky is in cgs units. It doesn't matter if you forgot the exact value of the constant, I want the units.
- 1c. (5 pts) The paper gives a velocity coverage of 107.5 km/s in Section 2.1. Show how that follows from the stated observational parameters.
- 1d. (5 pts) What is meant by "Brightness Temperature", T<sub>B</sub>? How is it defined?
- 1e. (5 pts) There are two other temperatures named in the paper:  $T_k$  or kinetic temperature, and  $T_s$  or spin temperature. The latter is also called excitation temperature on page 1. Explain what is meant with each.
- **2**a.(5 pts) The paper talks a lot about Lyman  $\alpha$  photons in the introduction. What is the transition that gives rise to these photons? Derive its wavelength, given that the ionization of hydrogen from the ground state requires a photon with a minimum wavelength of 912Å.
- 2b. (5 pts) Why, if Lyman  $\alpha$  photons are present in the HI medium, is scattering of these photons a likely process?
- 2c. (5 pts) If a photon scatters, it is not destroyed but essentially absorbed and immediately re-e**f**mitted in a different direction generally. But there are two other processes (at least) that would destroy a Lyman α photon. What are they?
- **3.** These questions center on the basic method underlying the paper, which we discussed in ISM. The 21-cm emission coefficient does not depend on the kinenetic temperature of the gas. The best way to obtain information on that temperature is through HI absorption measurements. The goal is to determine the optical depth and spin temperature in the HI by observing a radio continuum source located behind the HI layer. It is then assumed that the

spin temperature equals the kinetic temperature. The procedure: measure the 21-cm emission next to a radio continuum source to obtain  $T_B(v)$  for the HI itself. Measure separately the continuum source brightness temperature in a frequency range just outside the HI line to get brightness temperature  $T_0$  for that source. Lastly, measure the brightness temperatures towards the continuum source across the frequency range of the HI line - the situation in problem 3c. This allows us to deduce the "absorption profile"  $(1 - e^{-\tau(v)})$ , as the authors call it and which they plot in Figure 1(b). One can then derive both  $T_k$  and optical depth  $\tau(v)$  from the data. Let's reproduce the radiative transfer that underlies the paper.

- a. (15 pts) Consider the HI spectrum for a single layer of gas at a kinetic temperature  $T_k$ . The layer is moving at a radial velocity  $v_0$  with respect to us. For the axes we use brightness temperature  $T_B(v)$  on the vertical axis to indicate the intensity and velocity,  $v_0$ , on the x-axis.
  - a.1 Make a sketch of the spectrum and mark  $v_0$ . Mark where 0 is on the vertical axis. Describe the line shape if the line is optically thin. What determines the FWHM of the line in the case of HI gas?
  - a.2 Optically thin implies that the optical depth is less than 1, so small, not necessarily zero. What would the figure look like if the optical depth were zero at all velocities (You might want to check your answer after question a.3 below).
  - a.3 What is the solution to the radiative transfer equation for this general situation of a single layer of 21-cm emitting gas at constant temperature  $T_K$ , so what is the expression for  $T_B(v)$  in terms of the kinetic temperature and the optical depth? a.4 Under which condition is the brightness temperature  $T_B(v)$  equal to the kinetic temperature, and at which velocity will this happen first?
- b. (5 pts) Why does the optical depth for HI increase as the kinetic temperature of the gas goes down? (There are two reasons but you will get full credit if you name either one).
- c. (10 pts) So let us now add a background radio continuum source which is observed through the layer of HI gas. The background source itself would have a brightness temperature  $T_0$  when observed in the frequency range just outside the spectral range of the HI line. You will now need to modify the solution you got in a.3.
  - c.1 Write the solution to the radiative transfer equation that applies in this case.
  - c.2 Make a sketch of the spectrum for that situation so a new figure in contrast to a.1. Be very careful in considering what happens at the location of the spectral line as you make your sketch in comparison to what you drew in Figure 2a. I need your vertical axis to be consistent in scale for the two cases, so I can tell if you considered the role of absorption in drawing your line profile. You may want to revisit your drawing after considering problem 3d.
- d. (10 pts) Now define the Equivalent Width of the HI line, first by a sketch. Copy your plot, from question 3c.2 and show the definition of EW in that plot, using the general concept of how an EW is defined for any spectral line. Then show that the EW is given by:

 $EW = [(T_k - T_0)/T_0] \int (1 - e^{-\tau(v)}) dv$ 

based on your solution in d. Discuss when the EW is negative and when it is positive.

e. (5 pts) Why do they use the Arecibo telescope to measure the HI brightness temperature away from the source, and not the VLA which they use to measure the HI spectrum towards the background source?

# EXCITATION TEMPERATURE OF THE WARM NEUTRAL MEDIUM AS A NEW PROBE OF THE Lylpha RADIATION FIELD

CLAIRE E. MURRAY<sup>1</sup>, ROBERT R. LINDNER<sup>1</sup>, SNEŽANA STANIMIROVIĆ<sup>1</sup>, W. M. GOSS<sup>2</sup>, CARL HEILES<sup>3</sup>, JOHN DICKEY<sup>4</sup>, NICKOLAS M. PINGEL<sup>1</sup>, ALLEN LAWRENCE<sup>1</sup>, JACOB JENCSON<sup>2,5</sup>, BRIAN L. BABLER<sup>1</sup>, AND PATRICK HENNEBELLE<sup>6</sup>

<sup>1</sup> Department of Astronomy, University of Wisconsin, Madison, WI 53706, USA; cmurray@astro.wisc.edu

<sup>2</sup> National Radio Astronomy Observatory, P.O. Box O, 1003 Lopezville, Socorro, NM 87801, USA

<sup>3</sup> Radio Astronomy Laboratory, UC Berkeley, 601 Campbell Hall, Berkeley, CA 94720, USA

<sup>4</sup> University of Tasmania, School of Maths and Physics, Private Bag 37, Hobart, TAS 7001, Australia

<sup>5</sup> Department of Astronomy, Ohio State University, 140 West 18th Avenue, Columbus, OH 43210, USA

<sup>6</sup> Laboratoire AIM, Paris-Saclay, CEA/IRFU/SAp—CNRS—Université Paris Diderot, F-91191 Gif-sur-Yvette Cedex, France

\*Received 2013 November 28; accepted 2014 January 3; published 2014 January 15

## **ABSTRACT**

We use the Karl G. Jansky Very Large Array to conduct a high-sensitivity survey of neutral hydrogen (H<sub>I</sub>) absorption in the Milky Way. In combination with corresponding H<sub>I</sub> emission spectra obtained mostly with the Arecibo Observatory, we detect a widespread warm neutral medium component with excitation temperature  $\langle T_s \rangle = 7200^{+1800}_{-1200}$  K (68% confidence). This temperature lies above theoretical predictions based on collisional excitation alone, implying that Ly\alpha scattering, the most probable additional source of excitation, is more important in the interstellar medium (ISM) than previously assumed. Our results demonstrate that H<sub>I</sub> absorption can be used to constrain the Ly\alpha radiation field, a critical quantity for studying the energy balance in the ISM and intergalactic medium yet notoriously difficult to model because of its complicated radiative transfer, in and around galaxies nearby and at high redshift.

Key words: ISM: clouds – ISM: structure

## 1. INTRODUCTION

Understanding physical conditions within the diffuse neutral interstellar medium (ISM) is essential for producing realistic models of star and galaxy formation. Ambient gas temperature and density are crucial input parameters for heating, cooling, and feedback recipes on all astronomical scales. While numerical simulations are becoming increasingly complex, details regarding neutral gas temperature distributions, shielding properties, essential feedback sources, and excitation processes are still very much under debate (Bryan 2007; Christensen et al. 2012). The excitation processes of the 21 cm line are especially important for interpreting radio signals from early epochs of cosmic structure formation (e.g., the cosmic dark ages and subsequent epoch of reionization), when neutral hydrogen dominated the baryonic content of the universe and facilitated the formation of the first stars and galaxies (Pritchard & Loeb 2012). To interpret 21 cm signals from the early universe, it is necessary to decouple astrophysical effects from cosmological effects which is likely best done by analyzing excitation processes in the local ISM.

Traditional ISM models contain two neutral phases, the cold neutral medium (CNM) and the warm neutral medium (WNM), individually in thermal and pressure equilibrium (Field et al. 1969; McKee & Ostriker 1977; Wolfire et al. 2003). Widely accepted theoretical properties of these phases in the Milky Way include a kinetic temperature of  $T_k \sim 40$ –200 K and a volume density of  $n({\rm H\,I}) \sim 5$ –120 cm<sup>-3</sup> for the CNM, and  $T_k \sim 4100$ –8800 K and  $n({\rm H\,I}) \sim 0.03$ –1.3 cm<sup>-3</sup> for the WNM (Wolfire et al. 2003).

A convenient tracer for neutral gas is the H I 21 cm line, originating from the hyperfine energy splitting caused by magnetic moment interactions between the hydrogen atom's electron and proton. The high optical depth of the CNM makes 21 cm absorption signatures easy to detect, even with low sensitivity observations (e.g., Lazareff 1975; Dickey et al. 1977, 1983; Crovisier et al. 1978; Payne et al. 1978; Braun & Walterbos 1992; Heiles & Troland 2003; Kanekar et al. 2003; Mohan et al. 2004; Roy

et al. 2006; Begum et al. 2010). The excitation temperature (or spin temperature,  $T_s$ ) of the CNM can be directly estimated by solving radiative transfer equations.

In contrast, the WNM is characterized by very-low peak optical depth and so measuring its spin temperature from absorption requires extremely high sensitivity,  $\sigma_{\tau} \leq 10^{-3}$ , and attention to systematic errors. Only two direct measurements of WNM spin temperature exist so far (Carilli et al. 1998; Dwarakanath et al. 2002). However, Carilli et al. (1998) observed absorption in the direction of Cygnus A, an exceptionally bright radio continuum source with a flux density of ~400 Jy, and achieved excellent sensitivity with orders of magnitude less integration time than is required for the majority of (>3 Jy) radio continuum sources. Less accurate are upper limits on  $T_k$  (and thus  $T_s$  since  $T_s \leqslant T_k$ ) estimated by spectral linewidths (Mebold et al. 1982; Kanekar et al. 2003; Heiles & Troland 2003; Roy et al. 2013b) and approximate  $T_s$  estimates obtained by assigning a single temperature to strongly absorbing, complex H<sub>I</sub> profiles (Kanekar et al. 2011; Roy et al. 2013a).

Relating measured H<sub>I</sub> spin temperatures to model-predicted kinetic temperatures is further complicated by the uncertainty in the excitation mechanisms involved. The 21 cm transition in the high-density CNM is expected to be thermalized by collisions with electrons, ions, and other HI atoms, resulting in  $T_s \sim T_k$ . In contrast, low densities in the WNM imply that collisions cannot thermalize the 21 cm transition and therefore  $T_s < T_k$  (Field 1958; Deguchi & Watson 1985; Liszt 2001). However, the Lyα radiation field from Galactic and extragalactic sources can serve to thermalize the transition. This requires a very large optical depth and a large number of scatterings of Lyα photons to bring the radiation field and the gas into local thermal equilibrium. While the underlying atomic physics is understood (Wouthuysen 1952; Field 1958; Pritchard & Loeb 2012), the details of Ly $\alpha$  radiative transfer are complicated and depend on the topology and the strength of the Ly $\alpha$  radiation field, which are complex and poorly constrained in the multi-phase ISM (Liszt 2001).

To measure the physical properties of the WNM and the coupling between neutral gas and Ly $\alpha$  radiation, we are conducting a large survey, 21 cm spectral line observations of neutral gas with the EVLA (21 SPONGE), to obtain high-sensitivity Milky Way H I absorption spectra using the Karl G. Jansky Very Large Array (VLA). The recently upgraded capabilities of the VLA allow us to routinely achieve rms noise levels in an optical depth of  $\sigma_{\tau} \sim 7 \times 10^{-4} \ \mathrm{per} \ 0.42 \ \mathrm{km \ s^{-1}}$  channel, which are among the most sensitive observations of H I absorption to date. Currently, 24 out of 58 sightlines are complete after over 200 hours of observing time. This Letter summarizes our initial results from this project and the detection of the WNM using a newly developed analysis technique based on the spectral stacking of H<sub>I</sub> absorption and emission spectra. In Section 2, we summarize our observing and data processing strategies, results of the stacking analysis are provided in Section 3 and discussed in Section 4, and we present our conclusions in Section 5.

## 2. OBSERVATIONS AND DATA PROCESSING

## 2.1. Observations

Each source, selected from the NRAO/VLA Sky Survey (Condon et al. 1998), was chosen to have a 1.4 GHz flux density ≥3 Jy to avoid excessively long integration times with the VLA to reach the desired sensitivity. In addition, we select sources generally at high Galactic latitude ( $|b| > 10^{\circ}$ ) to avoid complicated CNM profiles associated with the Galactic plane and with angular sizes less than 1' to avoid resolving substantial flux density. All VLA observations use three separate, standard L-band configurations, each with one dual-polarization intermediate frequency band of width 500 kHz with 256 channels, allowing for a velocity coverage of 107.5 km s<sup>-1</sup> and resolution of 0.42 km s<sup>-1</sup>. We perform bandpass calibration via frequency switching, and all data were reduced using the Astronomical Image Processing System (AIPS). The absorption spectra,  $\tau(v)$ , were extracted from the final cleaned data cubes following calibration detailed in the 21 SPONGE pilot paper (Begum et al. 2010).

In addition, for each sightline we obtain H1 emission profiles which estimate the brightness temperature  $(T_B(v))$  in the absence of the radio continuum source. Of our 24 sightlines, 11 have emission profiles from the Millennium Arecibo 21 cm Absorption Line Survey (Heiles & Troland 2003), 10 have emission profiles from the Galactic Arecibo L-band Feed Array survey in H1 (GALFA-H1: Stanimirović et al. 2006; Peek et al. 2011), and for three sightlines which were not included in the Millennium survey or the GALFA-H1 survey to date, we use emission spectra from the Leiden—Argentine—Bonn (LAB: Kalberla et al. 2005) survey. Arecibo H1 emission spectra have not been corrected for contamination entering the telescope beam through distant sidelobes (so-called stray radiation).

# 2.2. Derivation of T<sub>s</sub> for Individual Components

To estimate  $T_s$  for individual spectral components, we follow the method of Heiles & Troland (2003). We first fit each absorption profile with Gaussian functions assuming thermal and turbulent broadening. We apply the statistical f-test to determine the best-fit number of components. We then fit the  $T_B(v)$  profile simultaneously for additional Gaussian components and  $T_s$  for each absorption-detected component by solving the radiative transfer equations discussed at length in Heiles & Troland



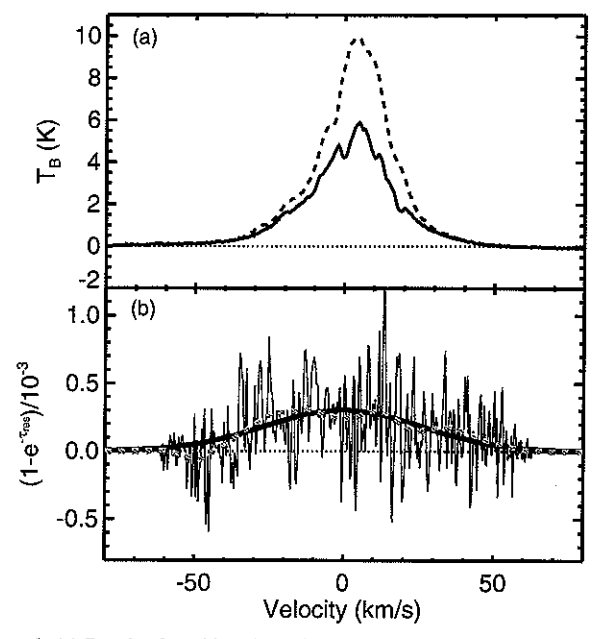


Figure 1. (a) Result of stacking the residual emission profiles  $T_{\rm B,res}(\nu)$  (solid line) for the 19 selected sources and the result of stacking the total emission profiles  $T_{\rm B}(\nu)$  (dashed line) for reference. (b) The result of stacking the residual VLA absorption profiles  $\tau_{\rm res}(\nu)$  (thin solid black) from the selected 19 sources. A smoothed version of the stack (10 km s<sup>-1</sup> boxcar kernel) is overlaid (dashed orange), with a simple Gaussian fit to the profile overlaid (thick solid green). Due to the fact that all shifted profiles do not cover the same velocity range, we add zeroes to the edges of each profile so that they cover the same range. This results in fewer non-zero channels in the farthest velocity bins, which causes the noise level to be lower there.

(2003). These results will be presented along with additional survey information in C. E. Murray et al. (2014, in preparation).

We next construct "residual" spectra to search for weak absorption features below our observational sensitivity by removing fitted models from the absorption and emission profiles. The best-fitting Gaussian components in absorption ( $\tau_i(v)$ ) where i denotes the ith component) are subtracted from each original absorption profile  $\tau(v)$  to produce a residual absorption spectrum,  $\tau_{\rm res}(v) = \tau(v) - \Sigma \tau_i(v)$ . The corresponding emission contribution from these components,  $\Sigma T_{s,i}(1-e^{-\tau_i(v)})$ , is removed from each emission profile to produce a residual emission spectrum  $T_{\rm B,res}(v) = T_{\rm B}(v) - \Sigma T_{s,i}(1-e^{-\tau_i(v)})$ . Each residual emission spectrum is dominated by signals from the WNM purely detected in emission. Correspondingly, each residual absorption spectrum,  $\tau_{\rm res}(v)$ , contains noise, model imperfections, and weak absorption components below our detection threshold.

To minimize the effects of model imperfections in our results, we exclude sources that have strong model-subtraction errors from our analysis using the following technique. We first calculate the expected noise profile of the absorption spectrum,  $\sigma_{\tau}(v)$ , for each source. Because the LAB survey uses antennas of comparable size to those of the VLA, we follow methods described by Roy et al. (2013a) to estimate  $\sigma_r(v)$  using LAB H<sub>I</sub> emission. We next produce probability distribution functions (PDFs) of  $\tau_{res}(v)/\sigma_{\tau}(v)$  and exclude from further analysis 5/24 sources whose PDFs deviate from a normal distribution at ≥97.5% confidence. The excluded sources are significantly contaminated by model-subtraction artifacts and lie at low Galactic latitude where lines of sight probe many velocity-blended H1 clouds, which complicates Gaussian modeling. Table 1 lists the source name,  $\sigma_{\tau}$  calculated per 0.42 km s<sup>-1</sup> velocity channel in off-line channels, a weighting factor described in Section 3, and Galactic coordinates.

Table 1
Source Information

Source information				
Name	$\sigma_{r}^{\;\;\mathbf{a}}$	$W=1/\sigma_{\tau}^{b}$	l	b
	$(\times 10^3)$	$(\times 10^2)$	(deg)	(deg)
4C32.44	1.5	2.7	67.240	81.049
4C25.43	0.9	4.5	22.464	80.991
3C286	0.7	5.8	56.527	80.676
4C12.50	1.3	3.1	347.220	70.173
3C273	0.6	6.7	289.945	64.358
3C298	0.8	5.1	352.159	60.667
3C225A	1.5	2.7	219.866	44.025
3C225B	3	1.3	220.010	44.007
3C345	1.3	3.1	63.455	40.948
3C327.1	1.4	2.9	12.181	37.006
3C147 <sup>c</sup>	0.4	10.1	161.686	10.298
3C154 <sup>c</sup>	0.9	4.5	185.594	4.006
3C410	1.9	2.1	69.210	-3.768
B2050+36c	2.3	1.8	78.858	-5.124
P0531+19	0.5	8.1	186.760	-7.110
3C111 <sup>c</sup>	0.7	5.8	161.675	-8.821
3C133	1.8	2.2	177.725	-9.914
3C138	0.9	4.5	187.403	-11.347
3C123 <sup>c</sup>	0.7	5.8	170.581	-11.662
3C120	1.1	3.7	190.373	-27.397
3C48	0.7	5.8	133.961	-28.720
4C16.09	0.8	5.1	166.633	-33.598
3C454.3	0.9	4.5	86.108	-38.182
3C78	4.1	1.0	174.857	-44.514

#### Notes.

## 3. STACKING ANALYSIS OF H<sub>I</sub> ABSORPTION AND EMISSION SPECTRA

We have performed a spectral "stacking" analysis on our 19 remaining residual spectra to search for extremely weak absorption signals from the diffuse WNM. We first apply a velocity shift to both the residual emission and absorption profiles to remove the effect of Galactic rotation and align any remaining signals at  $0 \,\mathrm{km}\,\mathrm{s}^{-1}$ . The velocity shifts are computed using the first velocity moment of the residual emission spectrum for each source, so that  $\Delta v = -\int T_{\rm B,res} v \, dv / \int T_{\rm B,res} \tilde{d}v$ . To maximize the signal-to-noise ratio of the stacked absorption spectrum, the weight, W, for each profile is given by  $W = \tau_{\rm res}/\sigma_{\tau}^2$ (Treister et al. 2011). However, as discussed in the previous section,  $\sigma_{\tau} \propto T_{\rm B}$ . For constant  $T_{\rm s}$ , we have  $\tau_{\rm res} \propto T_{\rm B}$ , and so the weight simplifies to  $W = 1/\sigma_{\tau}$ . We measure  $\sigma_{\tau}$  in the off-line channels of each profile, and list these values with the weights W, normalized by the sum over all n = 19 profiles,  $\sum_n W_n$ , in Table 1. The same weighting values were applied to the residual emission spectra.

The weighted profiles are averaged to produce the final stacked emission and stacked absorption spectra shown in Figure 1. The rms noise in the stacked absorption spectrum is  $\sigma_{\tau} = 2.6 \times 10^{-4}$ , calculated over a fixed range of channels (20 to 30 and -30 to -20 km s<sup>-1</sup>). This is 4.2 times more sensitive than the median rms noise calculated in the same velocity channels in the individual residual absorption profiles ( $\sigma_{\tau} = 1.15 \times 10^{-3}$ ).

The enhanced sensitivity enabled by stacking allows us to detect a weak and broad absorption component which has a velocity width and centroid consistent with the stacked *emission* signal (Figure 1). This gives confidence that the

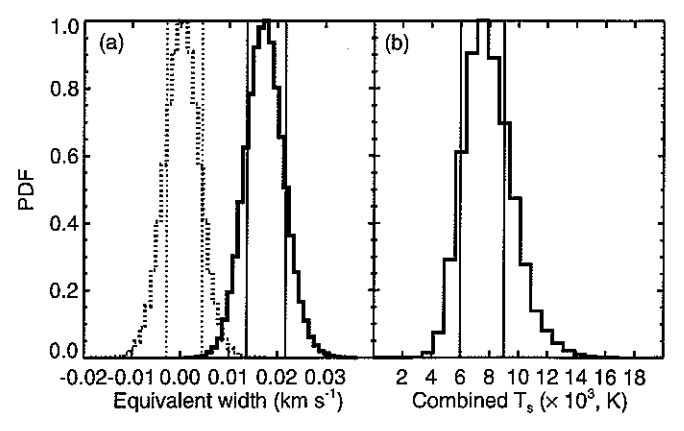


Figure 2. (a) PDF of stacked absorption EW following  $10^5$  iterations using a bootstrapping algorithm to select 19 sources from the total list of 19 with replacement, yielding  $\langle EW \rangle = 0.0182^{+0.0044}_{-0.0036} \, \mathrm{km \, s^{-1}}$  (68% confidence). To test that the signal is real, we invert (or multiply by -1) a random selection of half of the absorption residual profiles in  $10^5$  additional trials, yielding a distribution (dotted histogram) consistent with zero signal, as expected. Vertical lines denote  $10^5$ 0 uncertainty limits. (b) Distribution of spin temperatures from combining the PDFs of three different estimations (see text) computed in all  $10^5$  bootstrapping trials. The derived spin temperature is  $\langle T_s \rangle = 7200^{+1800}_{-1200} \, \mathrm{K}$  (68% confidence), with a 99% confidence lower limit of 4300 K.

stacked profiles trace physically related quantities. This broad absorption component is the weighted-mean,  $0\,\mathrm{km\,s^{-1}}$  centered absorption signal over all sightlines, and has an equivalent width (EW) within the velocity range common to all shifted profiles (-46 to  $30\,\mathrm{km\,s^{-1}}$ ) of EW =  $\int_{-46}^{30} (1-e^{-\tau_{\mathrm{res}}}) dv = 0.018\,\mathrm{km\,s^{-1}}$ . We next conduct a bootstrapping (see, e.g., Wall & Jenkins

2003) Monte Carlo simulation to estimate the integrated strength of the stacked absorption signal (Figure 1(b)) and test for contamination by outlier spectra. We run the stacking analysis on a new sample of 19 sightlines randomly chosen from our original 19 sightlines with replacement. We repeat this trial 10<sup>5</sup> times, each time recomputing the EW. The resultant normalized PDF of EWs (Figure 2(a), solid histogram) is nearly Gaussian, showing that the stacked EW signal is consistent with being drawn from a parent population of spectra with comparable means and not due to a few outlier spectra. The peak of the EW distribution and the numerically integrated 68% confidence limits are  $\langle EW \rangle = 0.0182^{+0.0044}_{-0.0036} \, \mathrm{km \, s^{-1}}$ , giving a 1 in 2 × 10<sup>6</sup> chance of being spurious (5 $\sigma$ ). Figure 2(a) also displays the result of repeating the bootstrapping simulation while inverting (or multiplying by -1) a random selection of half of the profiles (dotted histogram). The result is fully consistent with zero signal, verifying that our stacking method does not produce spurious detections.

Using the Monte Carlo bootstrapping method, we also constrain the FWHM and peak optical depth of the stacked absorption feature by a Gaussian fit as FWHM =  $50^{+15}_{-7} \,\mathrm{km}\,\mathrm{s}^{-1}$  and  $\tau_0 = 3.0^{+1.0}_{-0.4} \times 10^{-4}$  (at the central velocity of the feature,  $v_0$ ), respectively. Both quantities have well-defined, single-peaked distributions, suggesting that the detection is tracing a single gas component rather than a blend of many narrow components. We therefore proceed to estimate the typical spin temperature  $T_s$  of the gas detected in the stacked absorption spectrum.

We use three methods: (1)  $T_s = \int_{-46}^{30} T_{\rm B,res} dv / \int_{-46}^{30} (1 - e^{-\tau_{\rm res}}) dv$ , (2)  $T_s = T_{\rm B,res}(v_o)/(1 - e^{-\tau_{\rm res}})(v_o)$ , where  $v_o$  is the velocity at the peak of the smoothed stacked absorption signal, and (3) the methods of Heiles & Troland (2003), fitting a single Gaussian component to the absorption stack and solving for  $T_s$  by fitting this component to the emission stack without

<sup>&</sup>lt;sup>a</sup> rms noise in absorption profile calculated per 0.42 km s<sup>-1</sup> channel.

<sup>&</sup>lt;sup>b</sup> Normalized weighting factor (see Section 3);  $\Sigma_n W_n = 1$ .

<sup>&</sup>lt;sup>c</sup> Excluded sources (see Section 2.2).

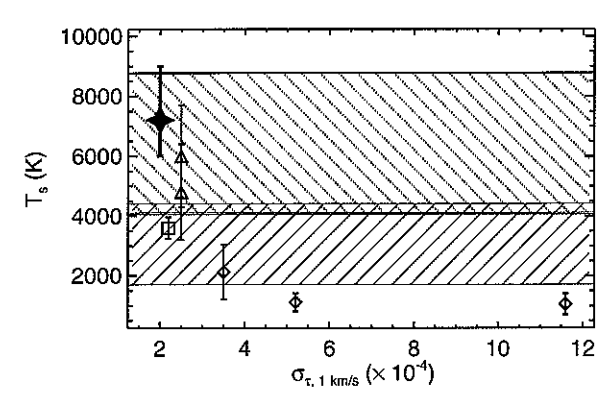


Figure 3. Comparison of previous  $T_s$  measurements for the WNM. Hollow symbols denote direct observational measurements of individual sightline components. Triangles: absorption toward Cygnus A (Carilli et al. 1998), square: absorption toward 3C147 (Dwarakanath et al. 2002), diamonds: 21 SPONGE absorption toward PKS0531+19, 3C298, and 3C133. All points are plotted vs. the rms noise in offi-line channels in the absorption profile, per 1 km s<sup>-1</sup> channel ( $\sigma_{\tau,1}$  km s<sup>-1</sup>). The purple dotted hatched region denotes the kinetic temperature range from Wolfire et al. (2003;  $T_k \sim 4100-8800$  K), and the blue hatched region denotes the spin temperature range from Liszt (2001) for all possible ISM pressures ( $T_s \sim 1800-4400$  K). The green filled star is the derived spin temperature from Figure 2(b), ( $T_s$ ) =  $7200^{+1800}_{-1200}$  K (68% confidence), with a 99% confidence lower limit of 4300 K.

additional components. For each of the  $10^5$  bootstrapping trials, we compute all three  $T_s$  estimates and combine their distributions to minimize systematic errors associated with any individual approach (Figure 2(b)).

We estimate a spin temperature of the detected absorption feature of  $\langle T_s \rangle = 7200^{+1800}_{-1200}$  K (68% confidence), with a lower limit at 99% confidence of 4300 K. We note that by shifting the residual profiles by the second velocity moment or by the location of maximum  $T_{\rm B,res}$ , we find consistent temperature estimates with similar significance. The possible contamination of stray radiation to the Arecibo H I emission spectra has no effect on the presence of the absorption stack, although it will tend to increase the EW of the emission stack and therefore increase the estimated  $T_s$  of the stacked feature. For the GALFA-H I survey, Peek et al. (2011) estimated that the level of stray radiation contamination is  $\leq 200-500$  mK, leading to an overestimate in our computed  $T_s$  of at most 13%. Therefore, the presence of stray radiation in our Arecibo H I emission spectra would not change our results.

## 4. DISCUSSION

In Figure 3, we plot all previous WNM  $T_s$  detections (open symbols) against the rms noise in off-line channels of the individual absorption spectra in which they were detected, with  $1\sigma$  error bars derived from line fitting. We exclude literature measurements which are estimated as upper limits from  $T_k$ or which assume single temperatures for multi-component sightlines. Our result from the stacking analysis (green filled star) is in agreement with measurements by Carilli et al. (1998, open triangles) obtained in the direction of the ~400 Jy bright Cygnus A. We emphasize that our result samples a widespread population detected from 19 sightlines, while Carilli et al. (1998) examine only a single direction. Our  $T_s$  estimate is significantly higher than all other direct measurements shown here. The trend of increasing  $T_s$  with increasing observational sensitivity confirms the expectation that previous experiments with lower sensitivity ( $\sigma_{\tau} \ge 5 \times 10^{-4}$ ) were unable to detect WNM with  $T_s > 1000 \,\mathrm{K}$  due to its low optical depth.

The range of predicted *kinetic* temperatures from the most detailed ISM heating and cooling considerations, shown by the dotted purple hatched region in Figure 3, is  $T_k \sim 4100-8800$  K (Wolfire et al. 2003). We use models considering only collisional excitation from Liszt (2001, their Figure 2) to show that under all plausible ISM pressures, the range of spin temperatures implied by this  $T_k$  range from Wolfire et al. (2003), is  $T_s \sim 1800-4400$  K (solid blue hatched region in Figure 3). Our measurement indicates that the mean spin temperature of the WNM is higher than expected theoretically for collisionally excited H I at 98% confidence.

Resonant scattering of Ly $\alpha$  photons can contribute enough to 21 cm excitation to allow  $T_s = T_k$ , as long as a sufficient fraction of the Ly $\alpha$  radiation permeates the WNM (Liszt 2001; Pritchard & Loeb 2012). However, the degree to which this can occur in a multi-phase ISM depends on several observationally unconstrained quantities: the local and external Ly $\alpha$  field, interstellar pressure, interstellar turbulence, ionization fraction, and the topology of the ISM. Using models from Liszt (2001), which assume a column density of hydrogen nuclei equal to  $10^{19}$  cm<sup>-2</sup> and the temperature of the Ly $\alpha$  radiation field being equal to the kinetic temperature, our  $T_s$  measurement constrains the fraction of Galactic flux from early-type stars which permeates H I clouds to  $> 1 \times 10^{-4}$ .

Our work provides the first observational evidence for the Ly $\alpha$  mechanism acting throughout the bulk of the Galactic WNM. By increasing observational sensitivity to  $T_s$  in comparison with expectations for  $T_k$ , stacking can be used to constrain the importance of non-collisional excitation on HI, as well as the origin and intensity of the Ly $\alpha$  radiation field. In the future, 21 SPONGE will obtain more absorption sightlines to increase our sensitivity to weak underlying signatures of the WNM, thereby further refining these temperature constraints and sampling different Galactic environments.

# 5. CONCLUSIONS

We have presented the discovery of a weak ( $\tau_0 = 3.0^{+1.0}_{-0.4} \times 10^{-4}$ ), broad (FWHM =  $50^{+15}_{-7}$  km s<sup>-1</sup>) WNM absorption feature in the stacked absorption spectrum of 19 independent Galactic sightlines from the 21 SPONGE survey. Using Monte Carlo simulations, we have estimated the feature's spin temperature to be  $\langle T_s \rangle = 7200^{+1800}_{-1200}$  K, which is significantly (98% confidence) higher than theoretical predictions based on collisional excitation alone, likely due to the thermalization of H I by resonant Ly $\alpha$  scattering. This work provides the first observational evidence that the Ly $\alpha$  excitation mechanism is acting throughout the bulk of the Galactic WNM and demonstrates that the Ly $\alpha$  radiation field, a quantity that is difficult to measure yet vitally important for interpreting H I signals from early epochs of cosmic structure formation, can be probed using measurements of the WNM.

We thank an anonymous referee for helpful comments and suggestions. This work was supported by the National Science Foundation (NSF) Early Career Development Award AST-1056780. C.M. acknowledges support by the NSF Graduate Research Fellowship and the Wisconsin Space Grant Institution. S.S. thanks the Research Corporation for Science Advancement for their support. We thank A. Begum for help with initial survey observations, D. Able for developing initial data reduction strategy, and H. Liszt, J. S. Gallagher, N. Roy, and T. Wong for helpful discussions. The National Radio Astronomy

Observatory (NRAO) is a facility of the NSF operated under cooperative agreement by Associated Universities, Inc. J.J. was supported by the Research Experience for Undergraduates (REU) program at NRAO through a grant from the NSF. The Arecibo Observatory is operated by SRI International under a cooperative agreement with the NSF (AST-1100968) and in alliance with Ana G. Méndez-Universidad Metropolitana and the Universities Space Research Association.

## REFERENCES

Begum, A., Stanimirović, S., Goss, W., et al. 2010, ApJ, 725, 1779
Braun, R., & Walterbos, R. A. M. 1992, ApJ, 386, 120
Bryan, G. 2007, in EAS Publications Series, Vol. 24, Chemodynamics: From First Stars to Local Galaxies, ed. E. Emsellem, H. Wozniak, G. Massacrier, J.-F. Gonzalez, J. Devriendt, & N. Champavert (Cambridge: Cambridge Univ. Press), 77
Carilli, C. L., Dwarakanath, K. S., & Goss, W. M. 1998, ApJL, 502, L79
Christensen, C., Quinn, T., Governato, F., et al. 2012, MNRAS, 425, 3058
Condon, J., Cotton, W., Greisen, E., et al. 1998, AJ, 115, 1693
Crovisier, J., Kazes, I., & Aubry, D. 1978, A&AS, 32, 205
Deguchi, S., & Watson, W. D. 1985, ApJ, 290, 578
Dickey, J., Kulkarni, S., van Gorkom, J., & Heiles, C. 1983, ApJS, 53, 591
Dickey, J. M., Salpeter, E. E., & Terzian, Y. 1977, ApJL, 211, L77
Dwarakanath, K. S., Carilli, C. L., & Goss, W. M. 2002, ApJ, 567, 940

Field, G. B. 1958, PIRE, 46, 240 Field, G. B., Goldsmith, D. W., & Habing, H. J. 1969, ApJL, 155, L149 Heiles, C., & Troland, T. 2003, ApJS, 145, 329 Kalberla, P., Burton, W., Hartmann, D., et al. 2005, A&A, 440, 775 Kanekar, N., Braun, R., & Roy, N. 2011, ApJL, 737, L33 Kanekar, N., Subrahmanyan, R., Chengalur, J. N., & Safouris, V. 2003, MNRAS, 346, L57 Lazareff, B. 1975, A&A, 42, 25 Liszt, H. 2001, A&A, 371, 698 McKee, C., & Ostriker, J. 1977, ApJ, 218, 148 Mebold, U., Winnberg, A., Kalberla, P. M. W., & Goss, W. M. 1982, A&A, Mohan, R., Dwarakanath, K., & Srinivasan, G. 2004, JApA, 25, 143 Payne, H., Dickey, J., Salpeter, E., & Terzian, Y. 1978, ApJL, 221, L95 Peek, J., Heiles, C., Douglas, K., et al. 2011, ApJS, 194, 20 Pritchard, J. R., & Loeb, A. 2012, RPPh, 75, 086901 Roy, N., Chengalur, J. N., & Srianand, R. 2006, MNRAS, 365, L1 Roy, N., Kanekar, N., Braun, R., & Chengalur, J. 2013a, MNRAS, 436, 2352 Roy, N., Kanekar, N., & Chengalur, J. 2013b, MNRAS, 436, 2366 Stanimirović, S., Putman, M., Heiles, C., et al. 2006, ApJ, 653, 1210 Treister, E., Schawinski, K., Volonteri, M., Natarajan, P., & Gawiser, E. 2011, Natur, 474, 356 Wall, J. V., & Jenkins, C. R. 2003, Practical Statistics for Astronomers (Cambridge: Cambridge Univ. Press) Wolfire, M., McKee, C., Hollenbach, D., & Tielens, A. 2003, ApJ, 587, 278

Wouthuysen, S. A. 1952, AJ, 57, 31

Cume 386 solutions: All the questions can be answered from the ISM course I taught last fall. I expect much trouble with the radiative transfer part which is why I try to talk them through it carefully.

- 1a. Given the wavelength, the frequency follows to be 1420 MHz. The primary beam width of the Arecibo dish would be given by 1.2 (lambda/D) or about 3'.
- 1b. A Jansky is a flux or "flux density" unit, since it is monochromatic. The units would be: erg cm<sup>-2</sup> s<sup>-1</sup> Hz<sup>-1</sup>.
- 1c. Section 2: the bandwidth is 500 kHz, which gives a velocity coverage of  $(500 \times 10^3 / 1420 \times 10^6)$  3x10<sup>10</sup> km/s = 106 km/s.
- 1d. The brightness temperature is defined as the temperature at which the observed intensity at a frequency equals the Planck black body intensity at that frequency. Given the nature of Planck functions at different temperatures, there is always only one temperature that reproduces a given intensity at some frequency.
- 1e. The kinetic temperature is the temperature of a medium corresponding to the motion of the particles. That is, if there is a well defined temperature, the particles would be moving according to the Maxwellian velocity distribution characterized by the kinetic temperature.

The excitation temperature is the temperature that describes the level population according to the Boltzmann equation.

question deleted

- 1f. Generally, the 21cm is excited and de-excited primarly by collisions and if the gas has a Maxwellian velocity distribution, the excitation temperature would then equal the kinetic temperature. For HI the excitation temperature is often called "spin temperature". The paper discusses the situation where collisions may not be sufficiently frequent to equalize the kinetic and spin temperatures because the gas density becomes very low in the Warm Neutral Medium.
- 2a. This is n=2 to n=1 transition for hydrogen. The wavelength follows from the  $1/n^2$  scaling of the energy levels, which implies 3/4ths of the energy going from the n=2 to n=1 transition compared to that of the n= $\infty$  to n=1 transition. So 1216 Å.
- 2b. Because the HI will sit in its ground-state (n=1) in the ISM and the cross-section for absorption of Lyman  $\alpha$  photons is very large.
- 2c. After absorption, the Lyman  $\alpha$  photon is generally re-emitted and therefore it can be scattered multiple times. However, upon absorption to n=2 it can land in

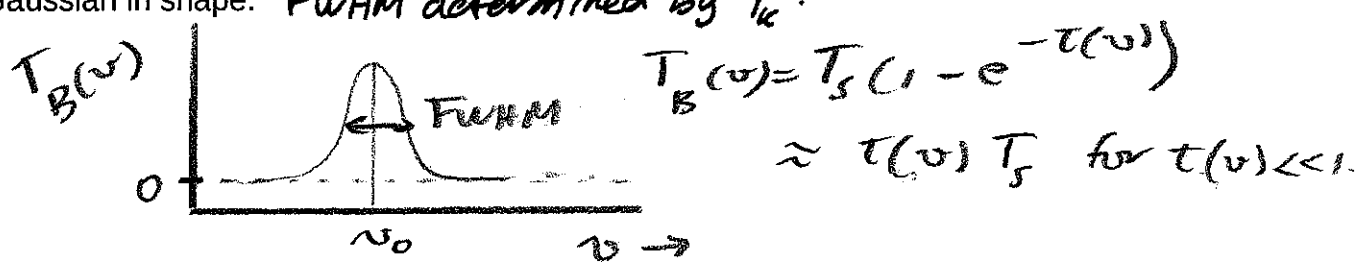
the atom

the meta-stable 2s state and the only way out of that is through a 2-photon continuum emission, which would destroy the Lyman  $\alpha$  photon. Another way to destroy the photon is through direct absorption by dust.

questur deleted

2d. The paper discusses this or hints at it. Upon emission of a Lyman  $\alpha$  photon the HI in the ground-state could find itself in either the upper or lower energy state for emission of a 21-cm photon. Thus, scattering of Lyman  $\alpha$  photons can change the population of the energy levels for the 21-cm photon.

3. a1. Key here: intensity zero outside the line, line centered at  $v_0$ , and line Gaussian in shape. FWHM deferm thed by  $T_w$ .



3a2. If the optical depth were zero, there would be no line, no signal.

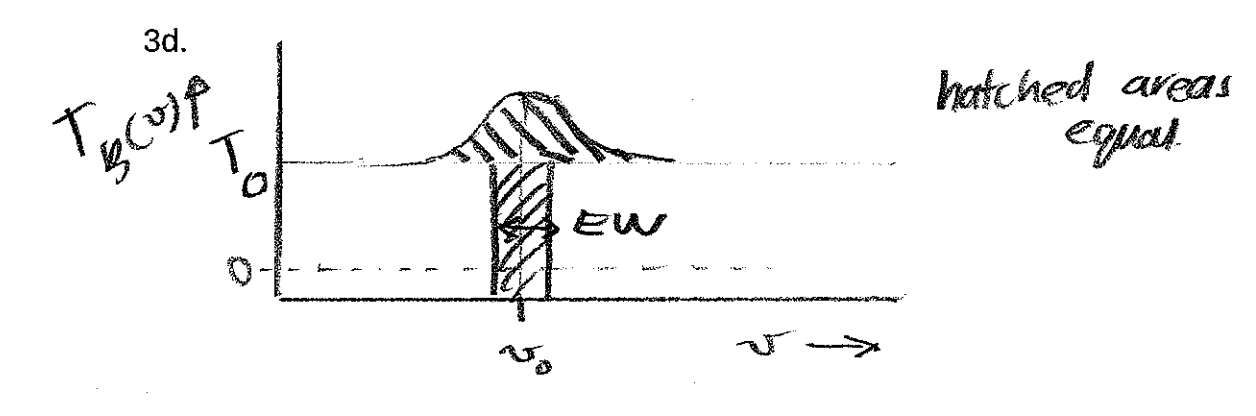
3a3.  $T_B(v) = T_s (1 - e^{-\tau(v)})$  A key point: include velocity dependence. We discussed this solution many times in ISM. If they forgot it, they can potentially recover it from the discussion in the paper or derive it from the radiative transfer equation.

 $3a4.\ T_B$  equals  $T_s$  for the optical depth going to infinity. This happens first in the line center.

3b. The optical depth is proportional to  $1/T_{\text{s}}$ . This follows from the expression for the absorption coefficient in terms of the Einstein B-coefficients, and the Boltzmann equation for the level populations. A simpler and second reason is that at colder temperatures the line will be narrower, so we pile up more of the total gas column density over a smaller velocity interval.

3c1. 
$$T_B(v) = T_0 e^{-\tau(v)} + T_s (1 - e^{-\tau(v)})$$

3c2. Key point: the line could be an emission line or an absorption line, depending on the value of  $T_0$  compared to  $T_s$ . But it should be LOWER in peak than sketched in 3a.1. Also, the continuum level should now be drawn at  $T_0$ .



This follows directly from the equations for the radiative transfer. The hatched area under the line in the spectrum drawn is equal to

$$T_0 e^{-\tau(v)} + T_s (1 - e^{-\tau(v)}) - T_0 = (1 - e^{-\tau(v)})(T_s - T_0)$$

The EW is defined as the integral over this but divided by T<sub>0</sub>.

3e. The VLA does not have short spacings and so it cannot measure extended structure. To get the HI emission itself we need to use a single dish with as narrow a beam as possible and measure the HI brightness temperature right next to the continuum source.